MICROWAVE POWER ABSORPTION PROFILE IN A CYLINDRICAL SAMPLE CONTAINED IN A RESONANT CYLINDRICAL CAVITY

H.W. JACKSON, M. BARMATZ, AND P. WAGNER
Jet Propulsion Laboratory, California Institute of Technology, Pasadena, CA 91109

ABSTRACT

An analytic approach is used for evaluation of the microwave power absorption profiles in a lossy dielectric cylinder coaxially aligned in a cylindrical cavity. This approach, based on a cylindrical shell model, also determines the normal mode frequencies and fields. Absorption profiles inside the sample will be presented for resonant modes that are intrinsically angular independent. In addition, results will be presented for special modes that are not intrinsically angular independent, but produce angular independent absorption for time average values. This new development broadens the class of modes that can be used in heating materials when isotropy about an axis is needed. We demonstrate how this model can extend the application of cavity perturbation theory for determining dielectric constants to cylinders of larger diameter. Implications of these results for microwave processing of materials are also discussed.

INTRODUCTION

The distribution of power absorption in a sample is a major factor that influences how materials undergo processing in a microwave cavity. This is mainly due to the effects of the power distribution on the temperature profile within a sample. Theoretical modeling can aid in matching absorption and temperature profiles to a process to attain optimum results in a variety of applications, including chemical vapor infiltration, sintering, fiber processing, combustion synthesis, joining, and annealing. Avoidance of catastrophic events such as thermal runaway or cracking due to thermal stresses in a sample during processing can also be aided by calculations and interpretation of the results.

We have previously applied a combination of analytic and numerical methods to calculate electromagnetic and thermal properties in spherical samples during microwave heating [1 - 4]. In the present work, we present a new approach to calculate the power absorption of a lossy dielectric cylindrical sample located on the axis of a resonant cylindrical cavity. This is a desirable geometry in many practical applications in processing materials. Furthermore, a system having this configuration can be treated theoretically with a high degree of accuracy within the framework of a cylindrical shell model that we have developed.

In this paper, we will focus on electromagnetic aspects of the problem and examine some power absorption profiles, Then we will discuss implications of calculated results for materials processing. In addition, we will illustrate how the model can be used in combination with experimental measurements of the resonant frequency and quality factor to determine the complex dielectric constant of a sample under some conditions. Data for dielectric constants as a function of temperature and frequency are not presently available for many materials of experimental interest. In these cases, the application of our model, in reverse, can determine the complex dielectric constant and provide input for calculations bearing more directly on materials processing. We are now combining results on power absorption distributions with a set of thermal equations to derive formulas for temperature profiles within cylindrical rods. We plan to conduct numerical studies of these profiles and report on them in the future.

The remainder of this paper is organized as follows. First, the theory of a cylindrical shell model is described. Next, calculated results are presented and discussed. Our conclusions are contained in the final section.

THEORY

The geometry of the model that we have used is shown in Fig. 1. The origin O of a cylindrical coordinate system (ρ, θ, z) is located at the center of the bottom plate of the cavity. The interior of the sample is treated as if it were partitioned into zones consisting of a central rod and many concentric tubes. The complex dielectric constant is taken to be uniform throughout each zone, but may vary from one zone to another. The temperature variation of the complex dielectric constant and the possibility that different materials may occupy different zones can be treated accurately with this model whenever normal mode fields in the loaded cavity have no z - dependence. The model can also yield accurate results for a general normal mode, even when there is z-dependence in the fields, whenever the temperature dependence of the complex dielectric constant can be neglected.

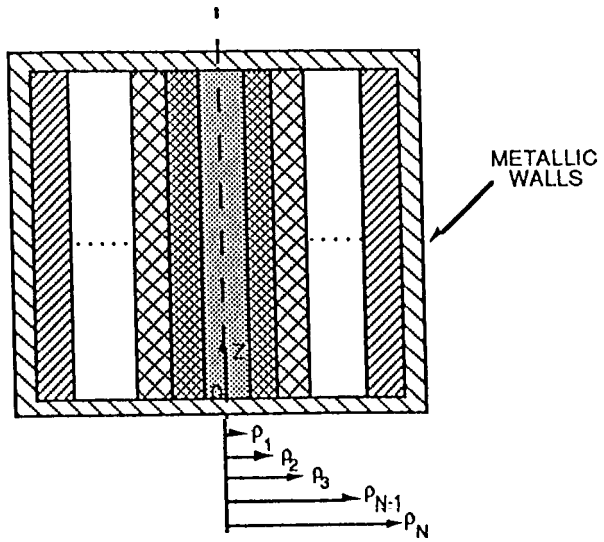

Fig. 1. Geometry of cylindrical rod and cavity.

Normal modes of this cylindrically loaded cavity are found by first writing down formulas for fields that are expressed as a superposition of basis functions that are known solutions of Maxwell's equations in each zone. Next, the appropriate boundary conditions are applied at the interior zone boundaries and at the cavity walls, including the end plates. After the boundary conditions are applied, the superposition still contains coefficients that must be determined. The problem of fixing those coefficients is solved using a 4 X 4 matrix representation with the aid of a technique that has been described by Sphicopoulos, Bernier, and Gardiol [5]. The normal mode frequencies and quality factors for the system are roots of a determinant of this 4 X 4 matrix. Both the determinant itself and its roots are complex-valued in general. We have developed an algorithm and a computer program for locating those roots to any specified degree of accuracy.

The complex-valued normal mode frequencies for the system are

$$\omega = \omega' - i\omega'' = \omega' - i\frac{\omega'}{2Q} \quad . \tag{1}$$

We have taken the time dependence of electromagnetic fields as e-ire'. In this case, the complex dielectric constant ε_j for zone j may be written as

$$\varepsilon_j \quad \varepsilon_0 \varepsilon_{r_j} = \varepsilon_0 (\varepsilon'_{r_j} + i\varepsilon''_{r_j}) , \tag{2a}$$

where

$$\varepsilon''_{r_j} = \frac{\sigma_j}{\omega' \varepsilon_0} . \tag{2b}$$

In Eq. (2), ε_0 is the permittivity of vacuum and σ_j is the electrical conductivity in ZOne j. In the present version of the theory, we have taken the cavity walls to be perfectly conducting, so they absorb no power. Therefore, the quality factor Q that appears in Eq. (1) is due to power absorbed by the sample only. Once a normal mode frequency has been located, coefficients in the linear combination of basis functions that represent the normal mode fields can be found by simple matrix

algebra. Having evaluated these coefficients for all of the zones, we have completely determined formulas for the normal mode fields throughout the cavity, including the interior of the sample.

The time average power absorbed per unit volume in the sample at point $\vec{r}$ in zone j, call it $\vec{P}_j$ (7), can then be evaluated using

$$\vec{P}_j(\vec{r}) = \frac{1}{2}\sigma\vec{E}_j(\vec{r})\bullet\vec{E}_j^*(\vec{r})\ . \qquad (3)$$

The asterisk denotes complex conjugation, and $\simeq$ (7) is the normal mode electric field. The power absorbed in each zone j can be evaluated analytically by integrating $\vec{P}_j$ over the zone. Calculations based on these formulas for normal mode frequencies, Qs, fields, and power absorption have been carried out. Illustrative results will be presented in the next section. In these calculations, only modes with no z - dependence in the fields are treated. For these cases, it turns out that the normal modes are all TM in character. Parenthetically, we should mention that for modes where there is z - dependence, the cylindrical sample produces mixed modes that are neither TM nor TE in character. The usual mode indices l, m, n, are applicable to the z - independent cases we will consider, where n = O.

The l = O modes are non-degenerate and have no angular dependence in the fields. The $l \neq$ O modes are doubly degenerate. The formula for the electric field in zone j at point $\vec{r}$ for one of the modes can be written as

$$\vec{E}_j(\vec{r}) = 2e^{il\theta}\left[c_l^j J_l\left(\lambda_j\rho\right) + d_l^j Y_l\left(\lambda_j\rho\right)\right]\ . \qquad (4)$$

The other mode contains a factor $e^{-il\theta}$ instead of $e^{il\theta}$. Provided that only one of these modes is excited, the power absorption distribution in the sample is independent of 0.

To excite only the $e^{il\theta}$ mode, for example, one can use two loop antennas with the normal to the plane of each loop in the θ - direction. (see Fig.2). The current in loop 2 is delayed by a phase factor $\pi/2$ with respect to loop 1, and the amplitude of the currents are equal. The angular separation between the antennas is given by

$$\bar{\theta}_0 = \left(\frac{4p+1}{2}\right)\frac{\pi}{l}\ , \qquad (5)$$

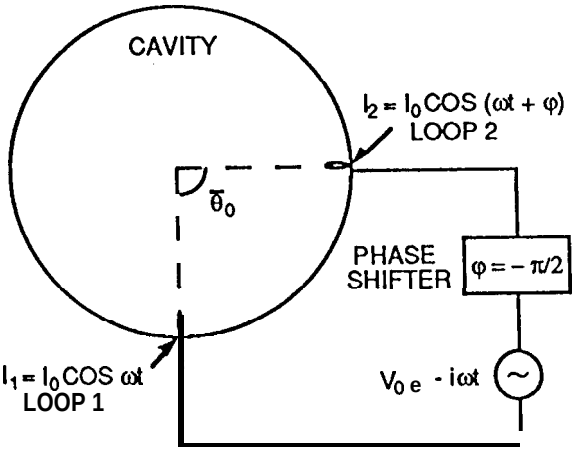

Fig. 2. Excitation of the $e^{il\theta}$ mode using two loop antennas

where p is an integer, O, 1, 2,. For the particular case where l = 1 andp=O, $\bar{\theta}_0 = \pi/2$. This case is shown in Fig. 1. The $e^{il\theta}$ modes open up additional frequencies and power absorption distribution that can be used in processing materials while maintaining isotropy about an axis. These modes are discussed in the next Section along with the l = O modes.

DISCUSSION

The absorption model was applied to cylindrical samples aligned along the axis of a cylindrical microwave cavity. The cavity was chosen to have a radius p_c = 4.69 cm and a length L = 6.63 cm. These dimensions correspond to $(L/2\rho_c) = \sqrt{2}$ and an empty cavity TM010 mode resonant

frequency fr = 2.45 GHz. For illustration purposes, we used rods of alumina with room temperature real and imaginary dielectric constants ε' = 9.0 and ε" = 0.0018, respectively. All rod calculations were performed using 100 evenly spaced zones.

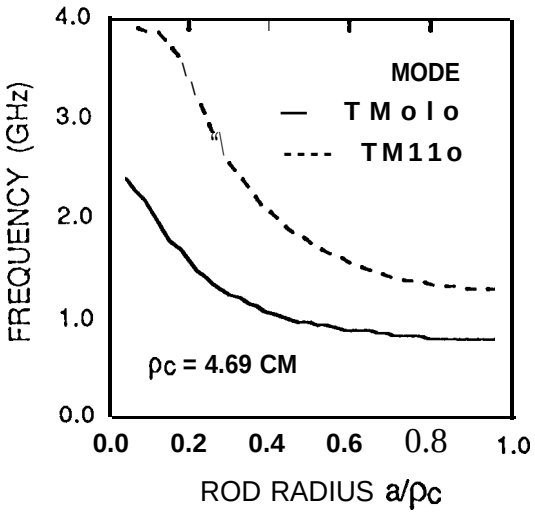

Fig. 3. Cavity resonant frequency versus rod radius.

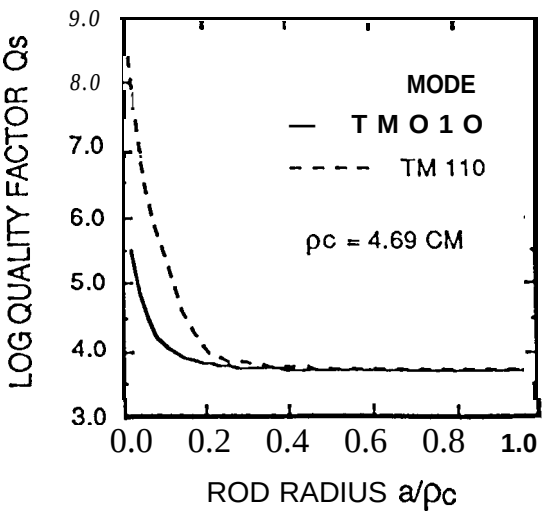

Fig. 4. Sample quality factor versus rod radius.

Figure 3 shows the dependence of the cavity resonant frequency on rod radius. As the rod radius, a, increases the resonant frequency decreases from the empty cavity value and approaches a limiting value at $a/\rho_c = 1$ corresponding to a fully loaded cavity. The ratio of the TM_{010} to TM_{110} cavity resonant frequencies, f_{010}/f_{110}, are equal for the empty and fully loaded cavity. However, the behavior of the resortant frequency in the partially loaded cavity depends on the internal electric field distribution within the rod which is mode dependent. The quality factor Q_s of the rod sample is the measure loaded cavity quality factor since we have assumed infinitely conducting walls. The dependence of Qs on the rod radius is shown in Fig. 4. The sample quality factor approaches infinity as the rod radius approaches zero. The TM_{110} mode is significantly less absorbing than the TM_{010} mode for aspect ratio's $a/\rho_c \leq 0.3$. For aspect ratio's $a/\rho_c \geq 0.3$ the sample Q's for both modes are essentially equal $Q_s = 5000$.

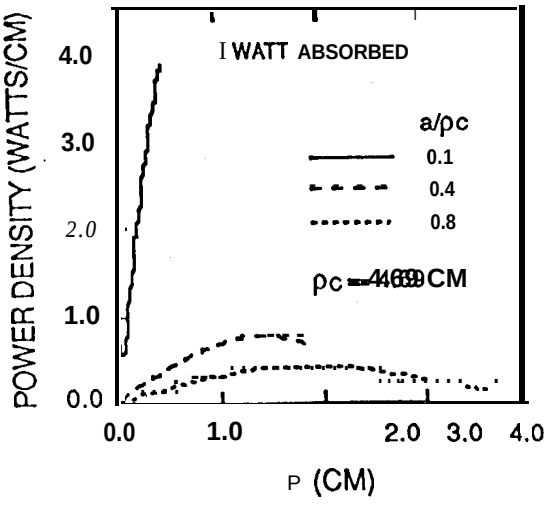

Fig. 5. TM_{010} mode power profile for rods of various radii.

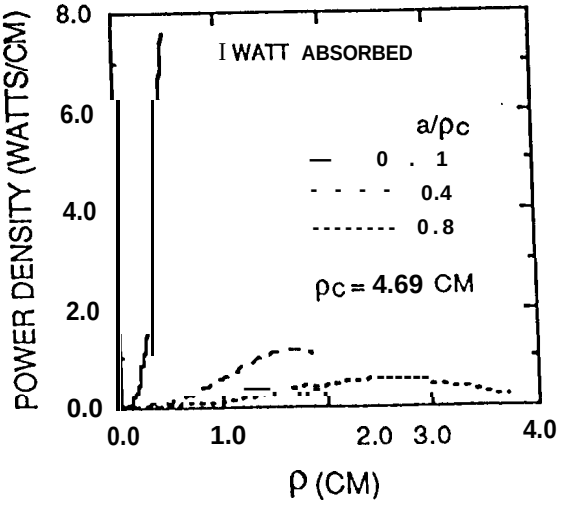

Fig. 6. TM_{110} mode power profile for rods of various radii.

The profile of the power absorption within a rod depends on the excitation mode and the rod radius to cylindrical radius aspect ratio. To illustrate the distribution of microwave power within rods of various radii, we have calculated the power absorbed per unit length assumed that a total of one watt is absorbed by each rod. In this way, we can compare the actual radial profiles between rods of different radii, since the area under the power density versus radius curve is one watt for every rod. Figure 5 shows the power density profile for the TM_{010} mode for rod radii corresponding to a/ρ_c = 0.1, 0.4, and 0.8. It is seen that the power density profile becomes steeper as the rod radius is reduced. The power density reaches a maximum inside the rod for larger radii, however the magnitude of the power density is reduced, The introduction of angular dependence into the mode changes the nature of the absorption near the center of the rod as seen in Fig. 6 for the TM I 10 mode. Here, there is a upward curvature of the power density near the center. This is in contrast with the downward curvature seen in Fig. 5 for the TM_{010} mode. The magnitude of the power density in the TM_{110} mode is almost doubled for the same size rod except near the center. A maximum in the power density is again obtained for the rods of larger radii. ‘

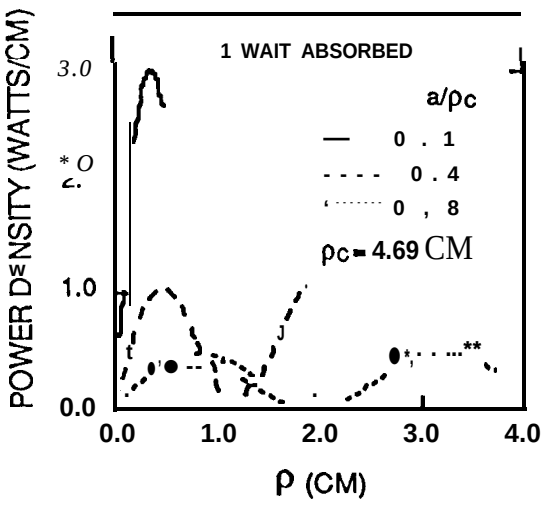

Fig. 7. TM_{020} mode power profile for rods of various radii.

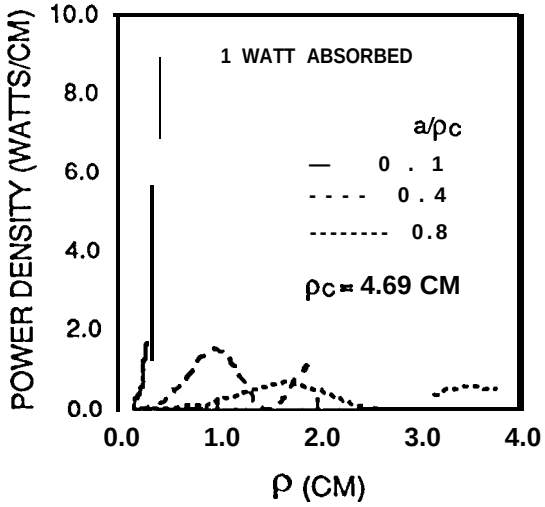

Fig. 8. TM220 mode power profile for rods of various radii.

The power density profile for the higher order TM_{020} and TM_{220} modes are shown in Figs. 7 and 8. An additional half wavelength radial oscillation is included within the cylindrical cavity by going from the TM_{010} mode to the TM_{020} mode. This additional oscillation in the cavity electric field also leads to oscillations in the power density profile within the rod. The amount of oscillatory behavior in a rod depends on the rod radius to cylindrical radius aspect ratio. Increasing the order of the Bessel function by going from the TM_{020} mode to the TM_{220} mode reduces the radial dependence of the electric field near the axis of the cavity. This effect causes the resultant power density profile within a rod to be streched out along the radial direction.

The cylindrical model developed here is capable of calculating the change in both the resonant frequency and quality factor of the cavity upon insertion of a cylindrical rod along the axis. We have compared the model calculations for the frequency shift and sample quality factor to the predictions of cavity perturbation theory [6]. For these calculations, we excited the microwave cavity in the TM_{010} mode and used the complex dielectric constants ε' = 10.0 and ε'' = 0.01 for the rod material. The calculated frequency shifts from the cylindrical model and cavity perturbation, shown in Fig. 9, overlap to better than 3 % for rod radii $a \leq 0.15$ cm ($a/\rho_c \leq 0.03$). In the range 0.15 cm < $a \leq$ 0.5 cm ($0.03 < a/\rho_c \leq 0.11$) the frequency shifts agree to within= 6.8 %. Above a = 0.5 cm, the calculated values diverge with cavity perturbation, predicting a larger decrease in the frequency shift. The log of the quality factor Qs calculated from the cylindrical model and cavity perturbation is shown in Fig. 10. For rod radii as 0.15 cm, the Q values agree

to within ≈ 8 %, while in the range O. 1S cm < a ≤ 0.5 cm the maximum disagreement in the Q's is 19%. As with the "frequency shift, the Q values diverge for a > 0.5 cm with cavity perturbation predicting a lower Q.

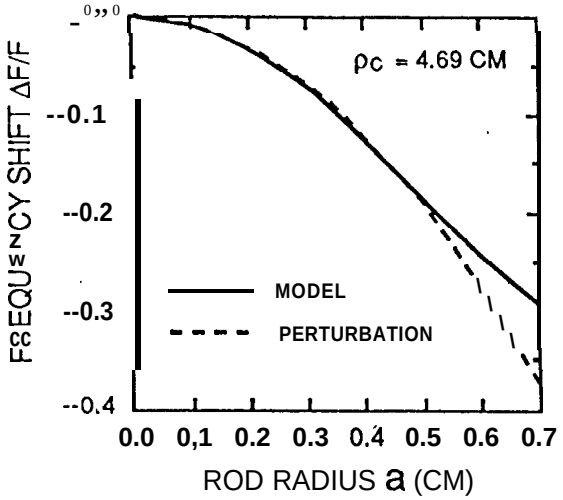

Fig. 9. TM010 "mode frequency shift versus rod radius for cylindrical model and cavity perturbation.

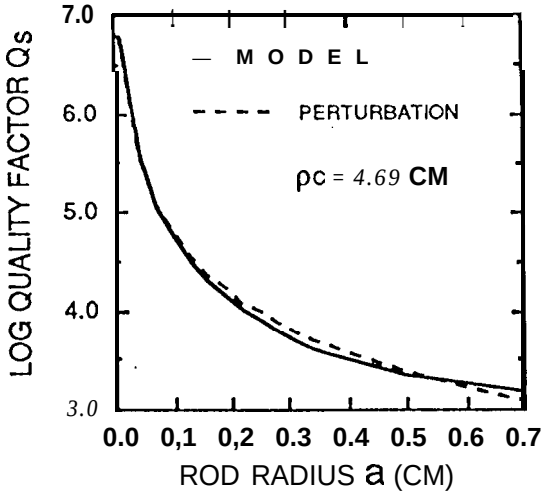

Fig. 10. TM010 mode sample quality factor versus rod radius for cylindrical model and cavity perturbation.

The above analysis indicates that, for a material with these typical dielectric constants, cavity perturbation will only be valid (to within 3 %) for rod radii a ≤ 0.15 cm, i.e., for ka <0.08. At a = 0.15, the sample quality factor Qs ≈ 33,000. This is a rather high Q value and would be hard to accurately measure experimentally. On the other hand, it would be much easier to apply the cylindrical model to measurements on a larger rod to extract the dielectric constants. For example, at a rod radius of a = 0.7 cm, the cylindrical model predicts a quality factor and frequency shift of Qs = 1560, and Af/f = -0.294, respectively, which are easy to measure experimentally. To illustrated the sensitivity of the cylindrical model in determining the dielectric constants, we

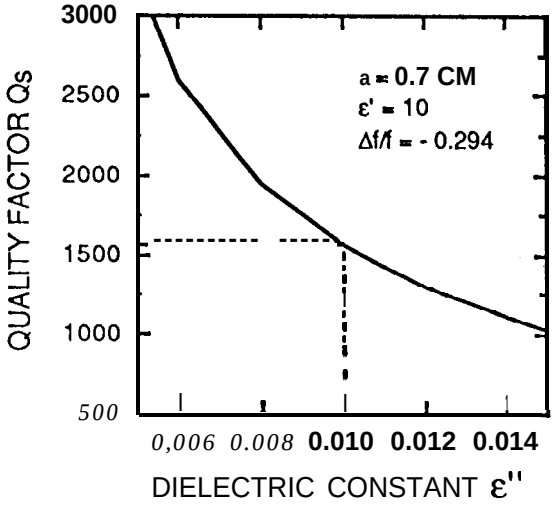

Fig. 11. Determination of ε'' using cylindrical model and experimental Qs.

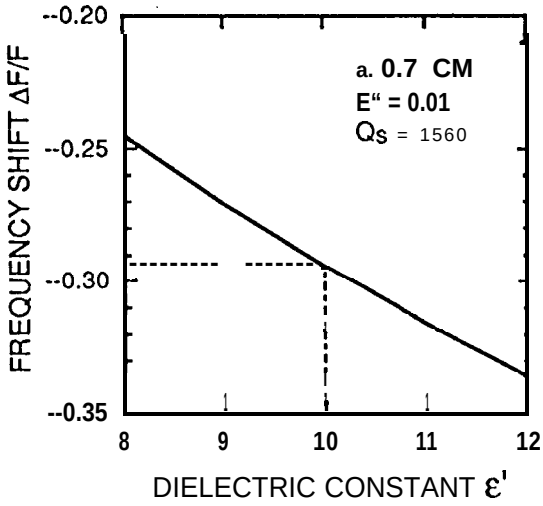

Fig. 12. Determination of ε' using cylindrical model and experimental Δf/f.

assumed the calculated Qs and Af/f for a = 0.7 cm are actually experimental values and used the model to calculate the required dielectric constants. Figure 11 shows the ε'' predictions of the theory for a range of Q_S about the values $\varepsilon' = 10$ and Af/f = 0.294, The sensitivity of the model is given by the slope at the intersection of the dashed lines, $\Delta\varepsilon''/\Delta Q_S = -6.1510-6$. A 10% uncertainty in AQs will yield a 10 % uncertainty in ε''. Figure 12 shows thee' predictions of the theory for a range of Af/f about the values $\varepsilon'' = 0.01$ and $Q_S = 1560$. Again the sensitivity of the model is given by the slope at the intersection of the dashed lines, $\Delta\varepsilon'/\Delta(\Delta f/f) = -44.1$. A 0.2 % uncertainty in $\Delta(\Delta f/f)$ will yield a 0.26 % uncertainty in ε'.

CONCLUSIONS

We have developed a microwave absorption model for a cylindrical rod situated along the entire axis of a cylindrical cavity. The model can be applied to modes with angular dependence for special excitation conditions. The power absorption profiles within various rods were calculated for the lower order $TM_{zm}o$ modes and the distribution of the power absorption was found to be dependent on the electromagnetic properties of the excitation mode, This mode dependence could have important consequences in efforts to control the thermal runaway process. We demonstrated that the cylindrical model is sufficiently sensitive to determine the complex dielectric constant from experimental quality factor and frequency measurements for large rod radii where the cavity perturbation technique is invalid.

ACKNOWLEDGMENT

The research described in this article was carried out at the Jet Propulsion Laboratory, California Institute of Technology, under contract with the National Aeronautics and Space Administration.

REFERENCES

1. H. W. Jackson and M. Barmatz, J. Appl. Phys. 70, 5193 (1991).
2. H.W. Jackson and M. Barmatz, Ceramic Transactions 21, 261, (1991).
3. M. Barmatz and H. W. Jackson, MRS Symp. Proc., Vol. 269, pp. 97-103 (1992).
4. H. W. Jackson, M. Barmatz and P. Wagner Ceramic Transactions, 36, 189, (1993).
5. T. Sphicopoules, L.-G. Bemier, and F. Gardiol, IEE Proceedings, Vol. 131, Pt. H, No.2, 94 (1984).
6. F.E. Borgnis and C.H. Papas, Encyclopedia of Physics 16, edited by S. Fluge (Springer, Berlin, 1958), pp411 -415.